Magnetic Gradient Scale Length

An Analysis of Why Certain Plasmas Require Close External Magnetic Coils

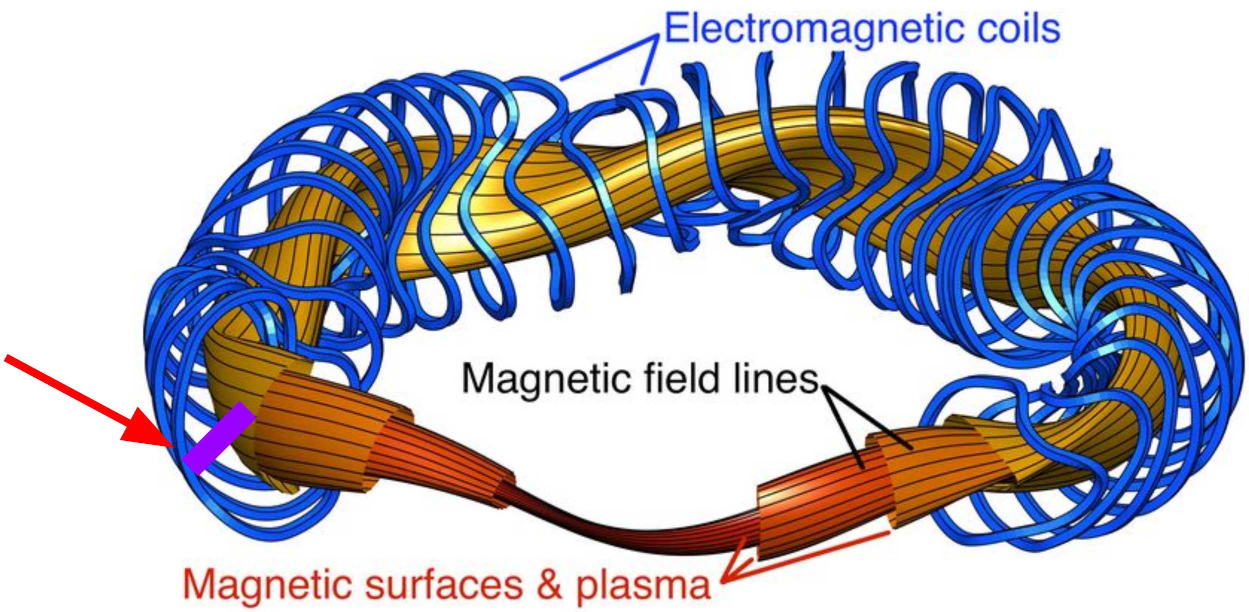

Pre-print:

By John Kappel

PI: Dr. Matt Landreman

Optimization of Stellarators is a Two Stage Process

Stage I Optimization

- Last Closed Flux Surface (LCFS) Shape
- Pressure Profile
- Rotational Transform

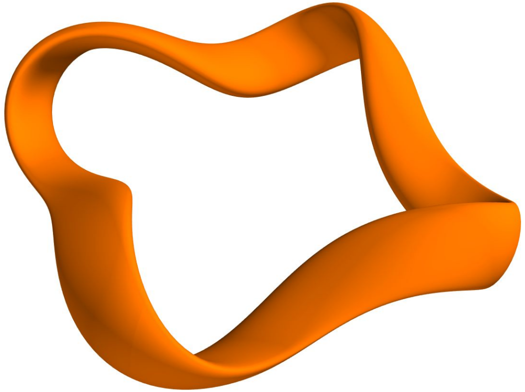

Stage II Optimization

- Coil Shape
- Subject to Engineering Constraints

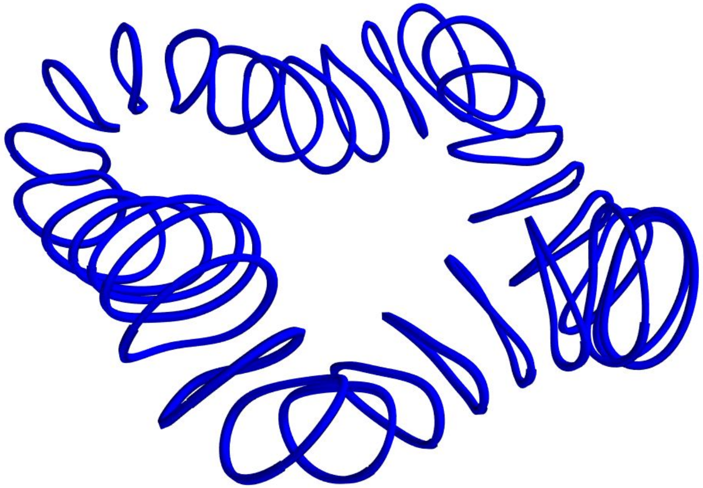

Stellarators Need Space for Breeding Blankets & Neutron Shielding

Need ~1.5 m between coils and plasma

Both ARIES-CS and W7-X report issues with not enough spacing

<u>Plasma-Coil Separation</u>: distance between the last closed flux surface and the center of an external field coil

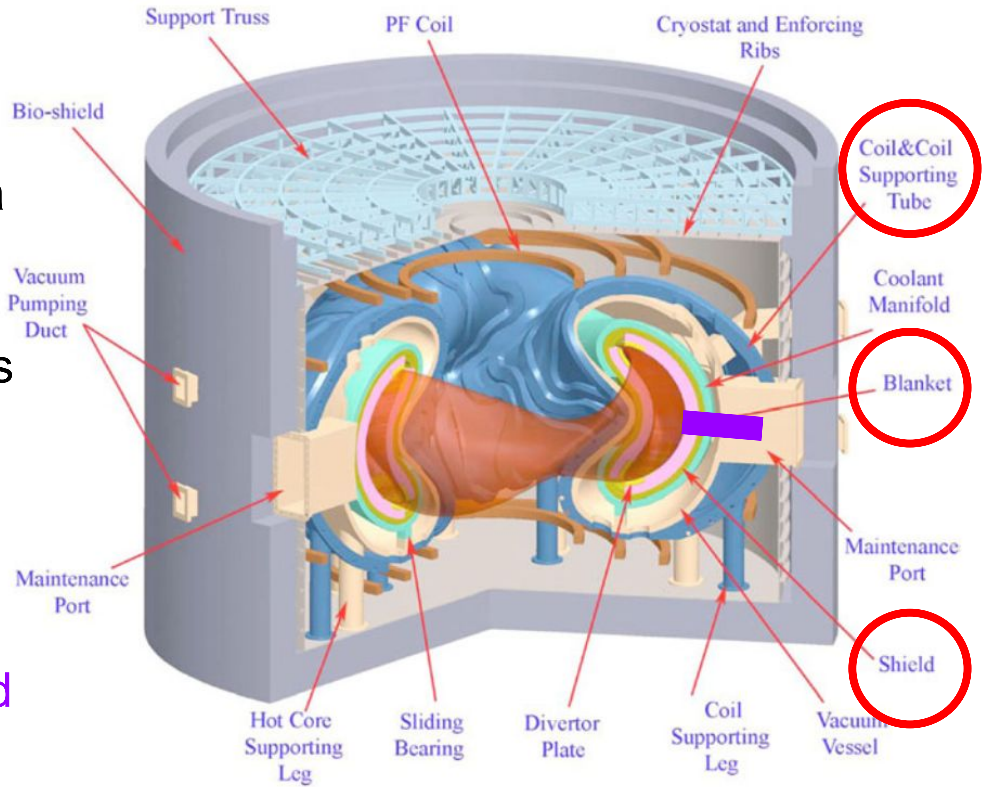

ARIES-CS Design from *The Aries-CS Compact Fusion Power Plant (2008)*

Other Benefits of Large Plasma-Coil Separation

1. Reduced coil ripple
2. Components can shift during startup and initialization
3. Plasma configurations large plasma-coil separation can be scaled down

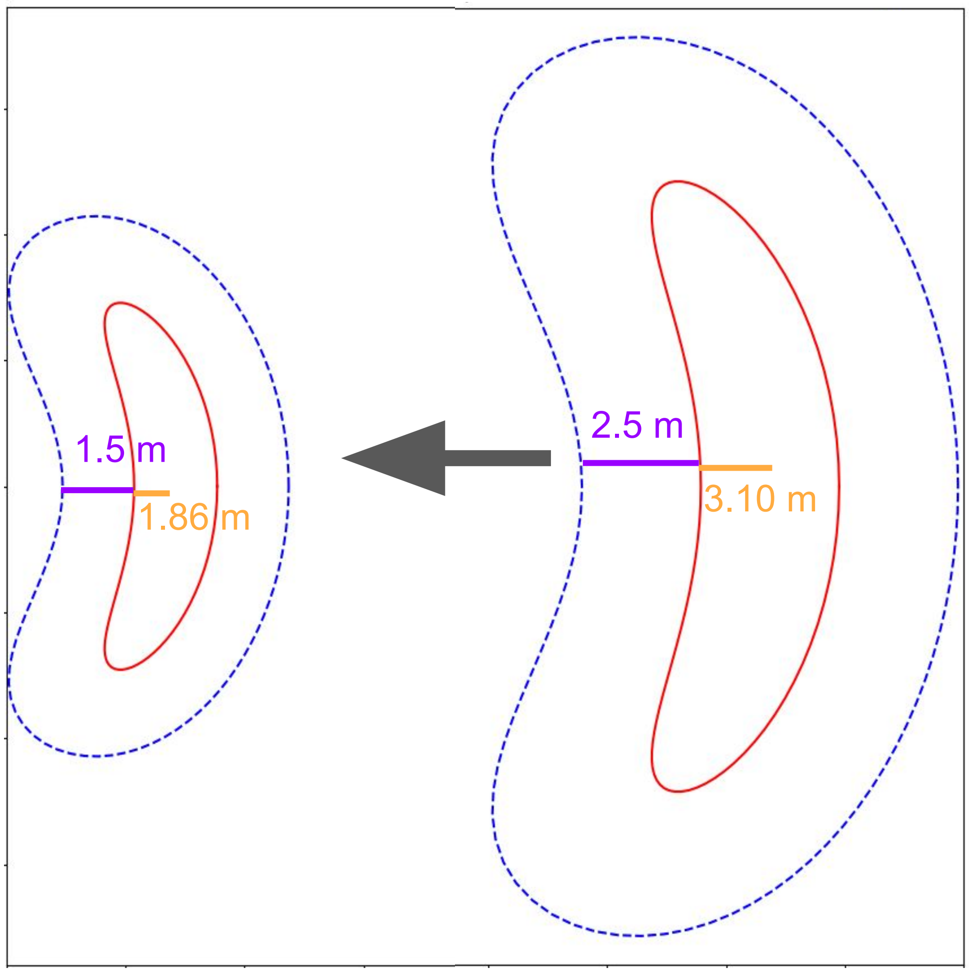

* Precise QH, to scale

Difficulty of Increasing Plasma-Coil Separation in Stage II Optimization

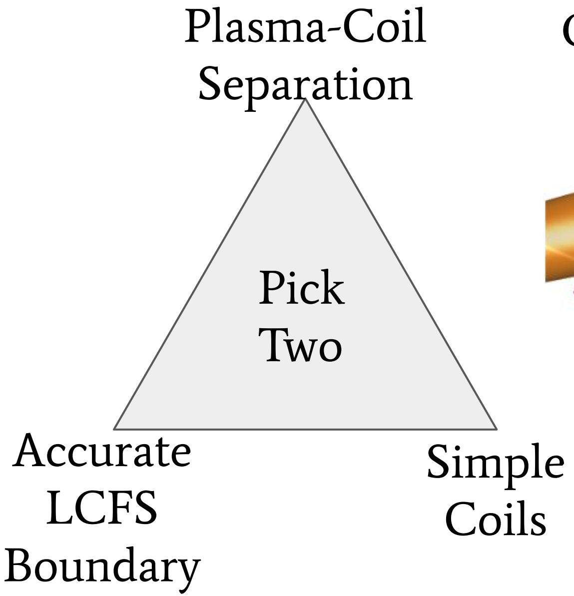

Coils offset a uniform distance from the W7-X plasma

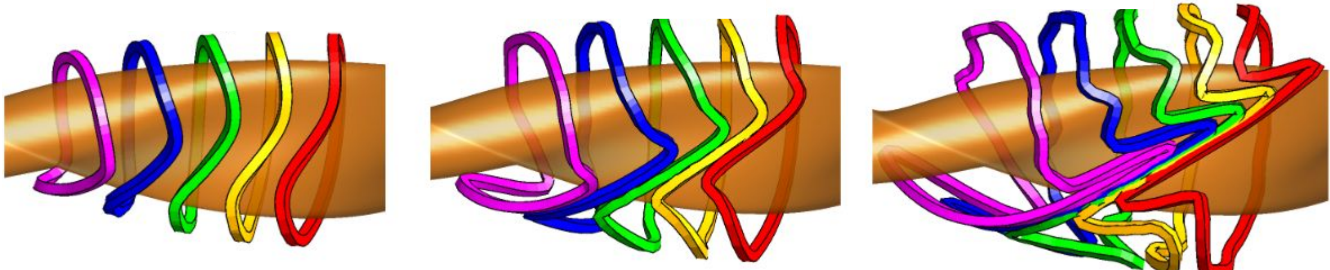

25 cm Separation   50 cm Separation   65 cm Separation

Coils that have a higher uniform separation from the plasma are more complex

Hypothesis: Plasma-Coil Separation can be Understood in Terms of Magnetic Gradient Scale Length

We shall show a **good correlation** between this magnetic gradient scale length ($L_{\nabla \mathbf{B}}$) and the plasma-coil separations of actual coil designs of over 40 configurations calculated in `REGCOIL`.

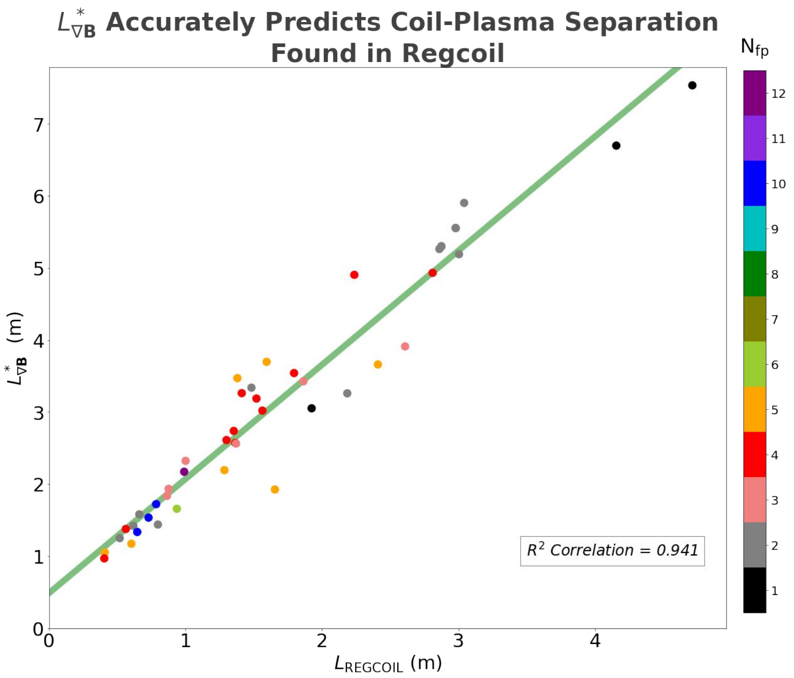

Outline

1. Intuition for Magnetic Gradient Scale Length
2. Methods of Coil Optimization in REGCOIL
3. Comparison Between $L_{\nabla \mathbf{B}}$ and $L_{\texttt{REGCOIL}}$ and Discussion

Outline

1. **Intuition for Magnetic Gradient Scale Length**
2. Methods of Coil Optimization in `REGCOIL`
3. Comparison Between $L_{\nabla \mathbf{B}}$ and $L_{\texttt{REGCOIL}}$ and Discussion

Precedent for the Magnetic Gradient Scale Length

L_{Te} → $$\frac{T_e}{||\nabla T_e||}$$

L_n → $$\frac{n}{||\nabla n||}$$

→ $$\frac{Q}{||\nabla Q||}$$

Arguments of scale lengths are used in plasma physics to determine which effects are negligible and significant.

A spatial gradient of the magnetic field encodes some information about the spatial distance from the coils to the plasma.

Magnetic Gradient Scale Length Has Been Used in Dipole Localization

For a **dipole:**

$$\mathbf{r} = -3(\nabla \mathbf{B})^{-1}\mathbf{B}$$

- Useful in RFID localization
    - single dipole-like field
- Cannot use for coil localization
    - multi-coil arrangement and not dipole-like

Conclusion: On the right track, but need a different equation!

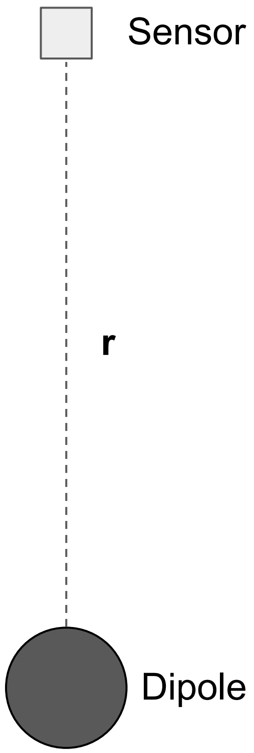

Nara et al. (2006) & Clark (2012)

Assumptions of ||∇B|| to Formulate $L_{\nabla B}$

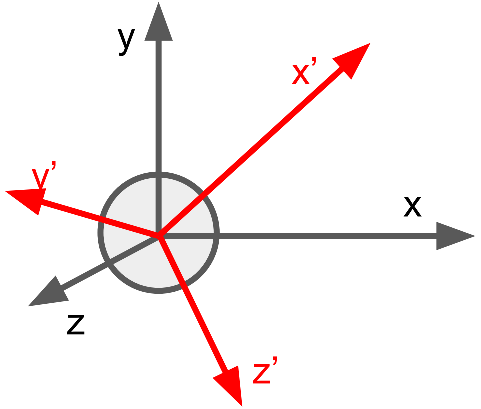

Many matrix norms exist. We should choose one so:

1. Norm uses all 9 components of gradient matrix
2. Norm is invariant to rotation

$$\|A\|_F = \sqrt{\sum_{i=1}^{m} \sum_{j=1}^{n} |a_{ij}|^2}$$

$$\nabla \mathbf{B} = \begin{bmatrix} \frac{\partial B_x}{\partial x} & \frac{\partial B_x}{\partial y} & \frac{\partial B_x}{\partial z} \\ \frac{\partial B_y}{\partial x} & \frac{\partial B_y}{\partial y} & \frac{\partial B_y}{\partial z} \\ \frac{\partial B_z}{\partial x} & \frac{\partial B_z}{\partial y} & \frac{\partial B_z}{\partial z} \end{bmatrix}$$

$$L_{\nabla \mathbf{B}} = \frac{\sqrt{2}B}{\|\nabla \mathbf{B}\|_F}$$

$L_{\nabla \mathbf{B}}$ Behavior In Model Geometry

$$\mathbf{B}(\rho) = \frac{\mu_0 I}{2\pi\rho}\hat{\phi}$$

$$\nabla \mathbf{B} = \frac{\mu_0 I}{2\pi}\left(-\frac{1}{\rho^2}\hat{\phi}\otimes\hat{\rho} - \frac{1}{\rho^2}\hat{\rho}\otimes\hat{\phi}\right)$$

$$\|\nabla \mathbf{B}\|_F = \frac{\sqrt{2}\mu_0 I}{2\pi\rho^2}$$

$$L_{\nabla \mathbf{B}} = \sqrt{2}\frac{B}{\|\nabla \mathbf{B}\|_F} = \rho$$

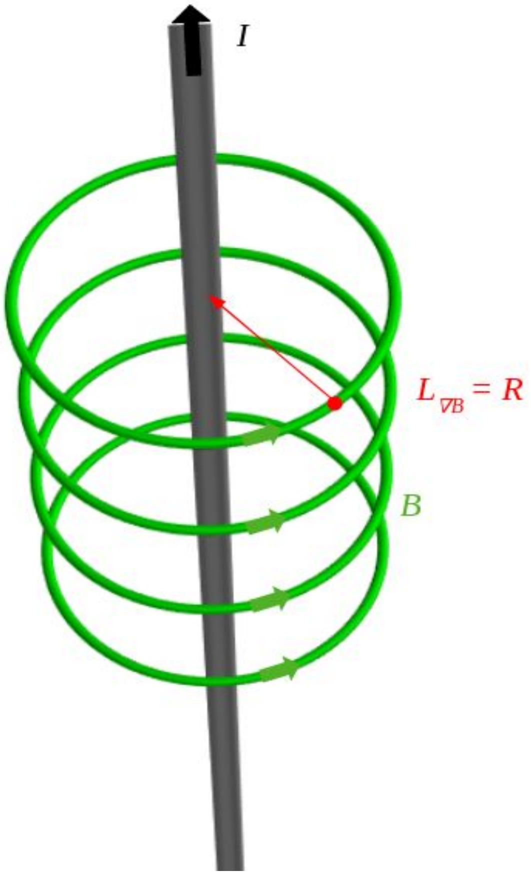

Outline

1. Intuition for Magnetic Gradient Scale Length
2. **Methods of Coil Optimization in `REGCOIL`**
3. Comparison Between $L_{\nabla \mathbf{B}}$ and $L_{\texttt{REGCOIL}}$ and Discussion

`REGCOIL` is a Useful Optimizer to Systematically Compare the Coils of Many Configurations

For any $\delta > 0$, there exists an infinite number of current arrangements in a finite region around the plasma that match **B** on the LCFS to an error $\varepsilon < \delta$.

`REGCOIL`’s objective function **preserves convexity**, so <u>any local minimum is a global minimum</u>.

Fewer tuning parameters than other codes.

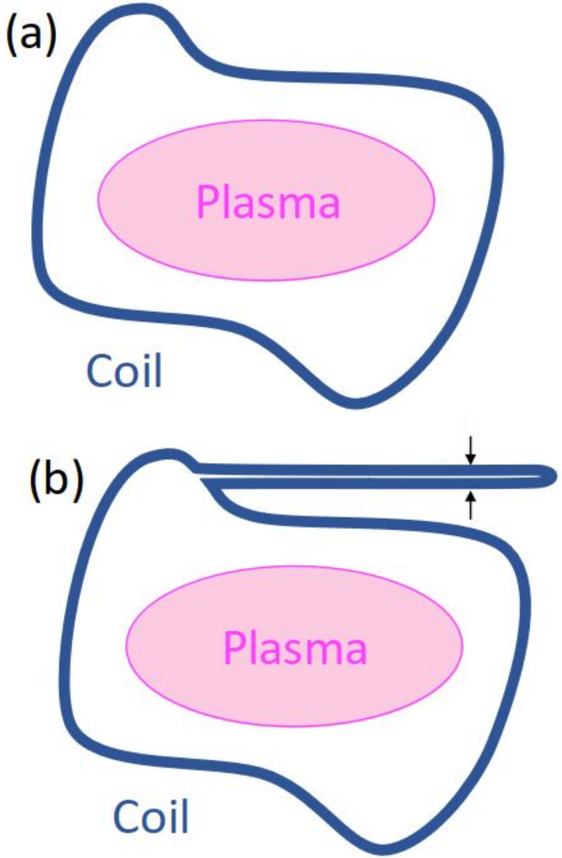

Overview of REGCOIL

$$\Phi'(\theta',\phi') = \sum_j \Phi_j \sin(m_j\theta' - n_j\phi') + \frac{G\phi'}{2\pi} + \frac{I\theta'}{2\pi}$$

$$\mathbf{K}' = \mathbf{n}' \times \nabla\Phi'$$

$$\mathbf{B}(\mathbf{r}) = \frac{\mu_0}{4\pi}\int d^2a' \frac{\mathbf{K}' \times (\mathbf{r}-\mathbf{r}')}{|r-r'|^3}$$

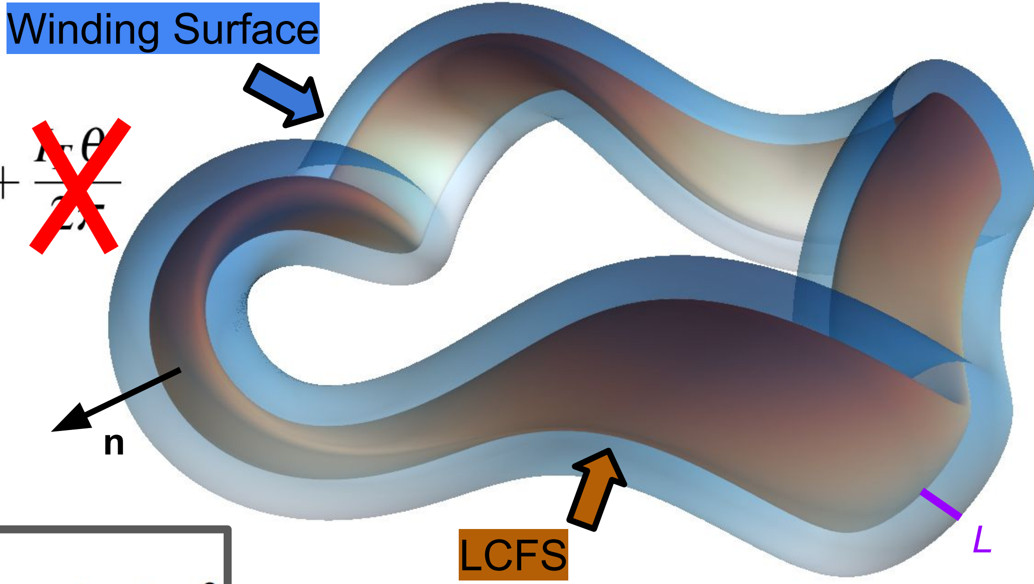

$$f = \int d^2a\, (\mathbf{B}(\theta,\zeta)\cdot\mathbf{n})^2 + \lambda \int d^2a'\, \|\mathbf{K}(\theta',\zeta')\|^2$$

2 free parameters: L and λ. A unique solution requires 2 constraints:

1. $B_{\mathrm{RMS}} = B^*_{\mathrm{RMS}}$
2. $||K||_\infty = ||K||^*_\infty$

B_{RMS} is a Measure of Accuracy in the Last Closed Magnetic Flux Surface

$$B_{\mathrm{RMS}} = \left(\frac{\int d^2a \, (\mathbf{B} \cdot \mathbf{n})^2}{A_{\mathrm{Plasma}}} \right)^{1/2}$$

B^*_{RMS} **uniquely** defines regularization parameter

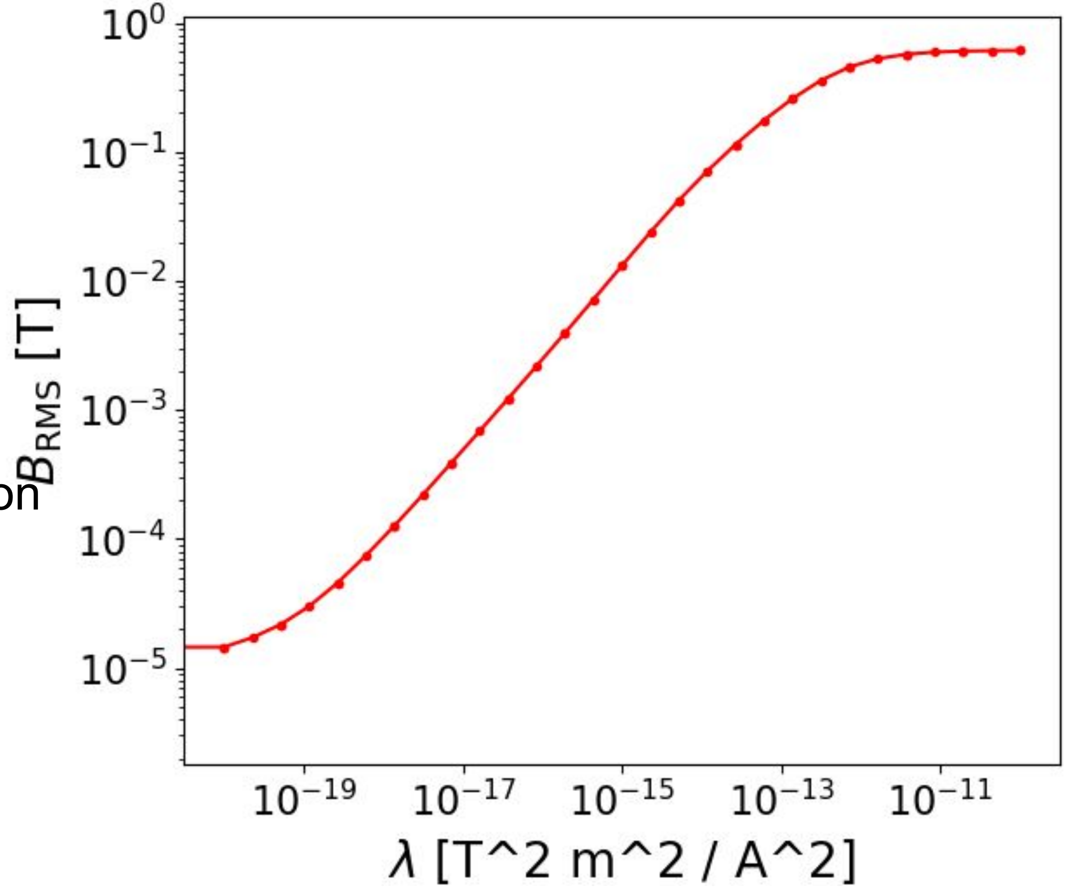

Smaller B_{RMS} = Better Flux Surfaces

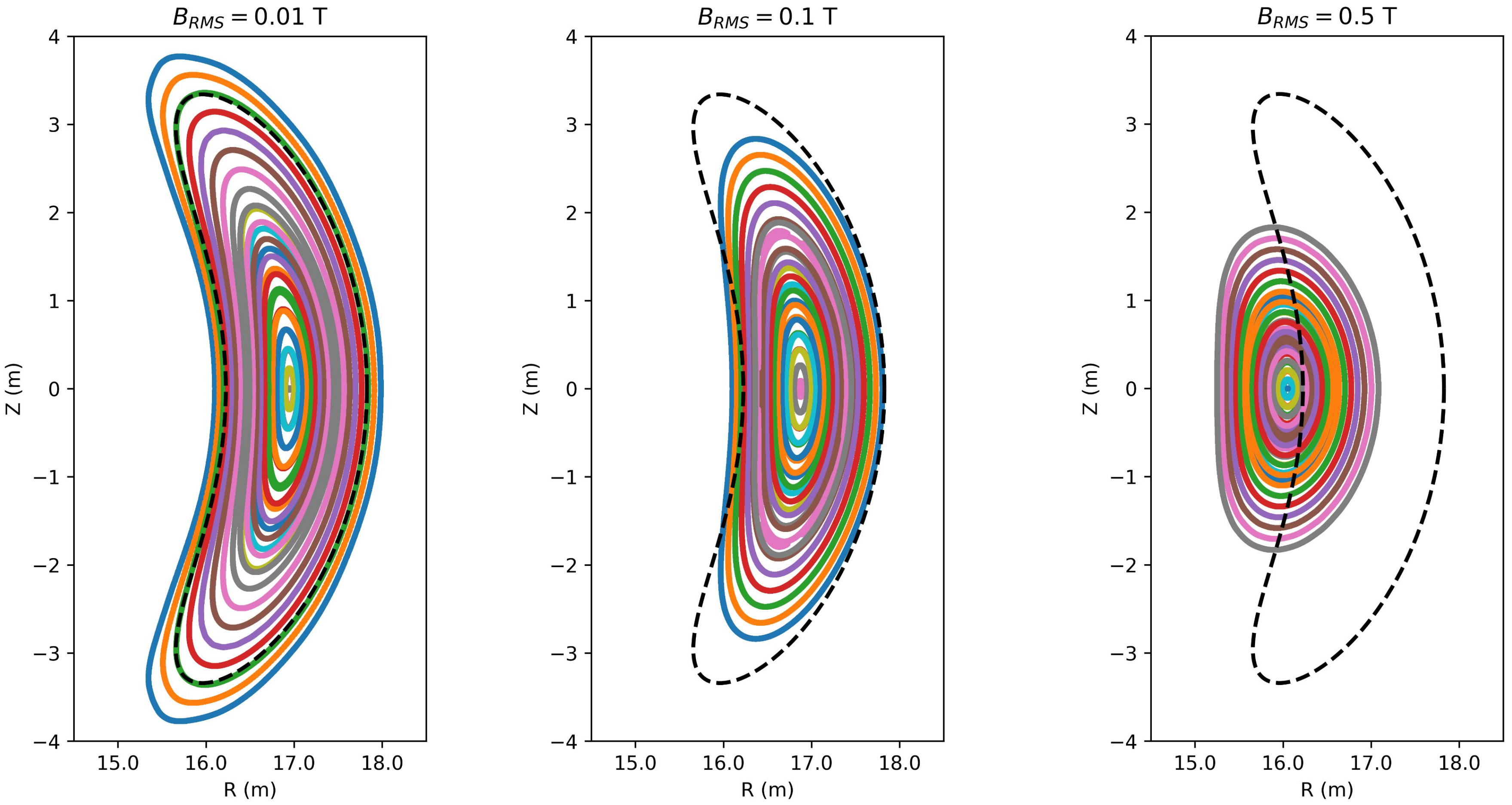

REGCOIL Must be Constrained by $||K||_\infty$ to make Buildable Coils

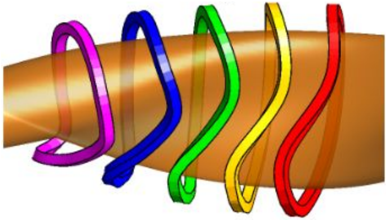

Low $||K||_\infty$

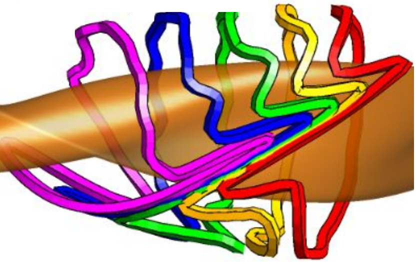

High $||K||_\infty$

$||K||_\infty$ or K_{max} is the **highest** current density on the winding surface

Uniquely defines plasma-coil separation

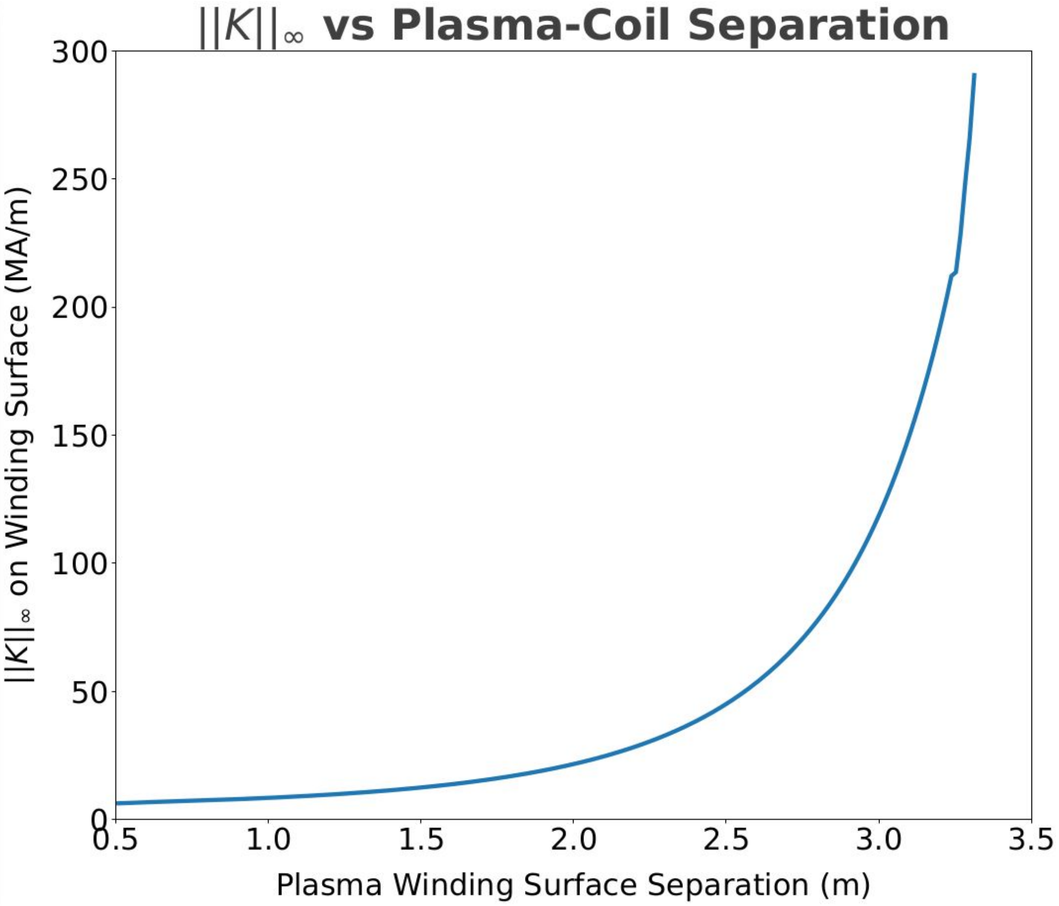

Virtual Casing Decomposes B_{coils} From B_{total}

$$\mathbf{B}(\mathbf{x}) = \mathbf{B}_{\text{plasma}}(\mathbf{x}) + \mathbf{B}_{\text{coils}}(\mathbf{x})$$

$$\mathbf{B}_{\text{coils}}(\mathbf{x}) = -\frac{1}{4\pi}\oint_{\delta\Omega} d^2a \frac{(\mathbf{n}\times\mathbf{B}\ \ (\mathbf{p}))\times(\mathbf{x}-\mathbf{p})}{|x-p|^3}$$

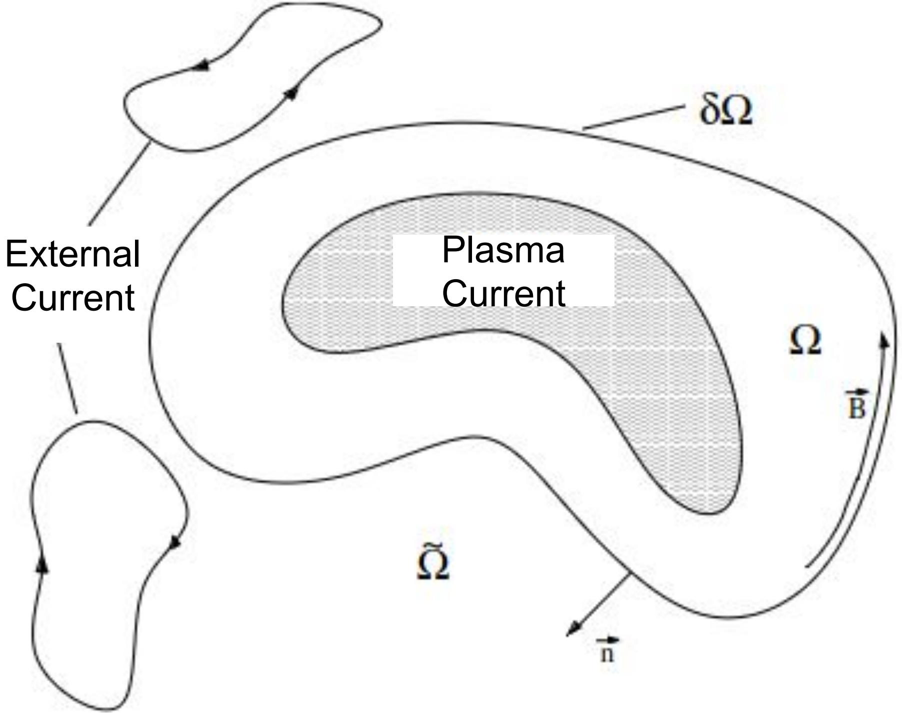

Code contribution by Dhairya Malhotra

Summary of Methods

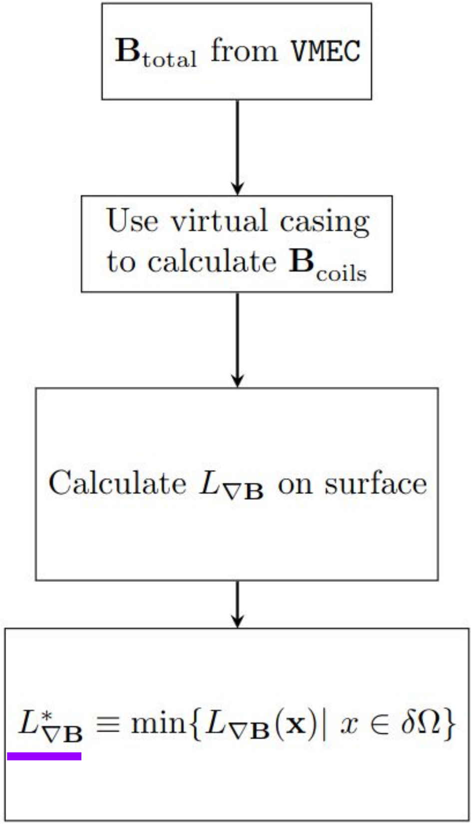

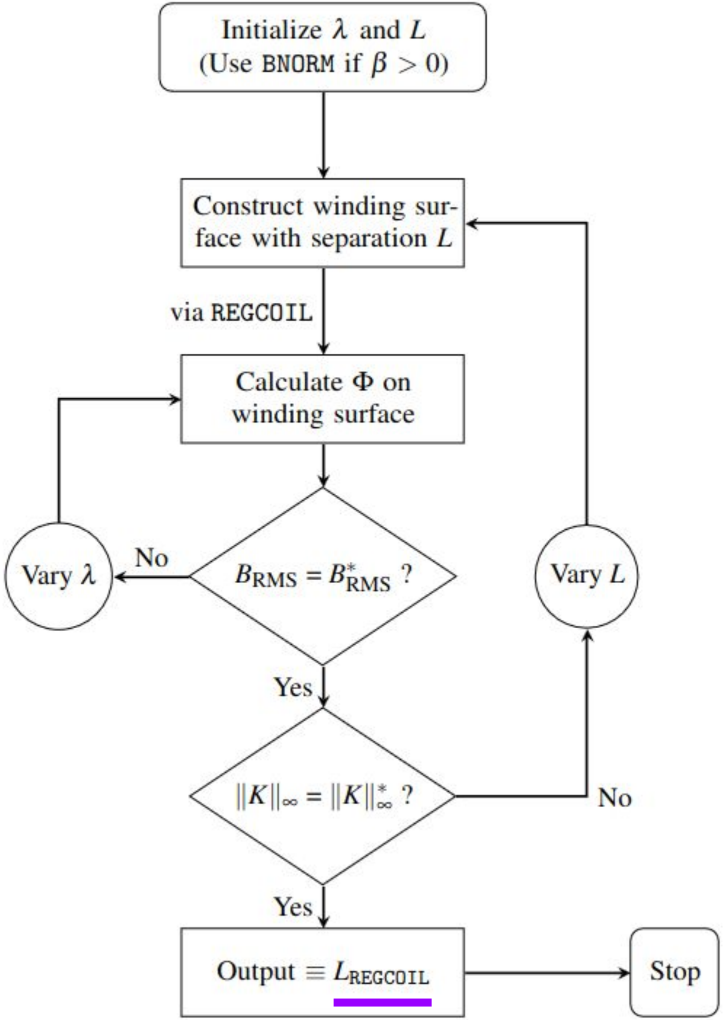

Outline

1. Intuition for Magnetic Gradient Scale Length
2. Methods of Coil Optimization in `REGCOIL`
3. **Comparison Between $L_{\nabla B}$ and L_{REGCOIL} and Discussion**

Parameters

- $B^*_{RMS} = 0.01$ T
- $||K||^*_\infty = 11.3$ MA/m
- a = 1.704 m
- $B_{Vol} = 5.865$ T
- mpol & ntor = 20
- n_θ & n_ζ = 96

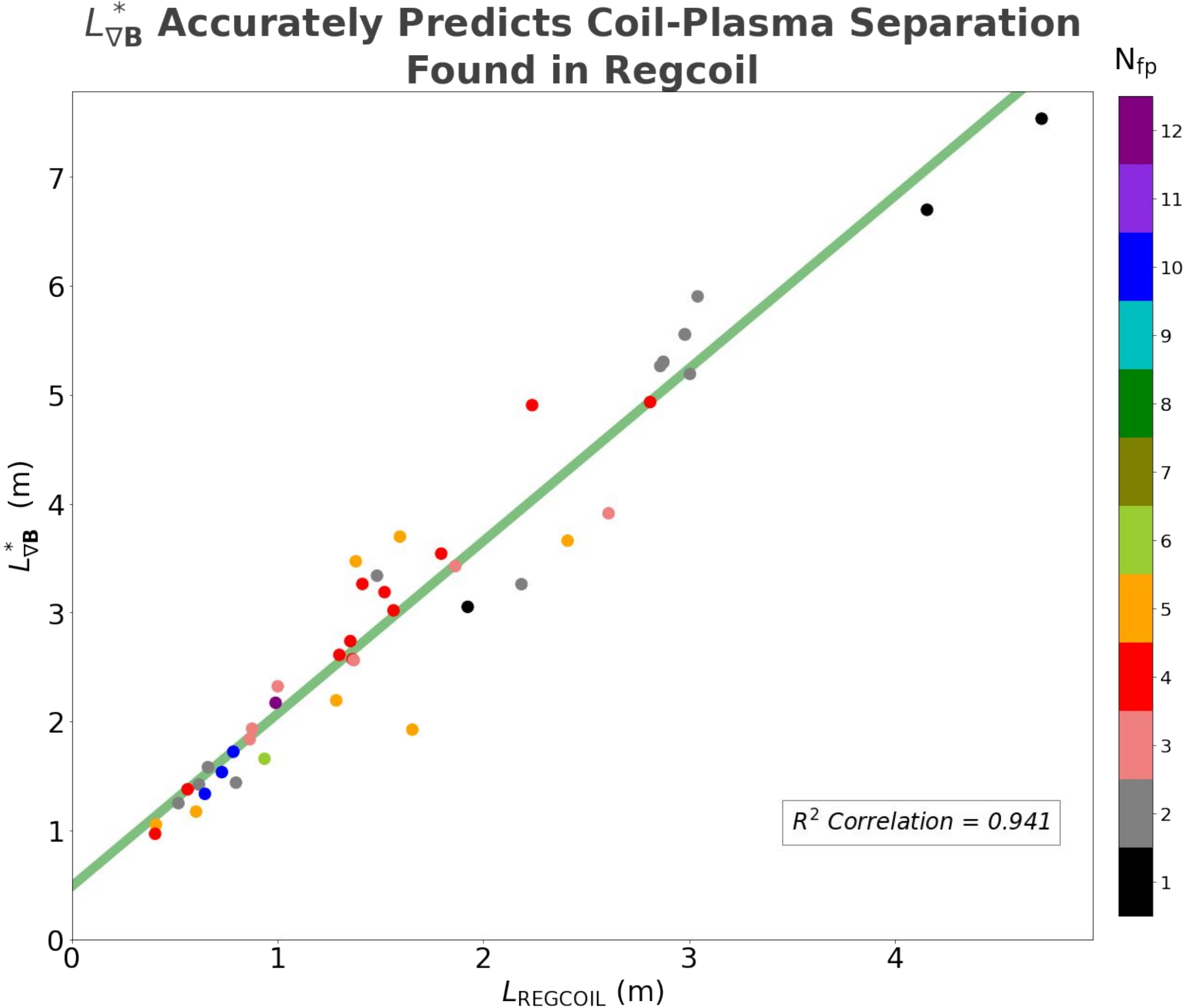

$L^*_{\nabla B}$ Accurately Predicts Coil-Plasma Separation Found in Regcoil

Parameters

- B^*_{RMS} = 0.01 T
- $||K||^*_\infty$ = 11.3 MA/m
- a = 1.704 m
- B_{Vol} = 5.865 T
- mpol & ntor = 20
- n_θ & n_ζ = 96

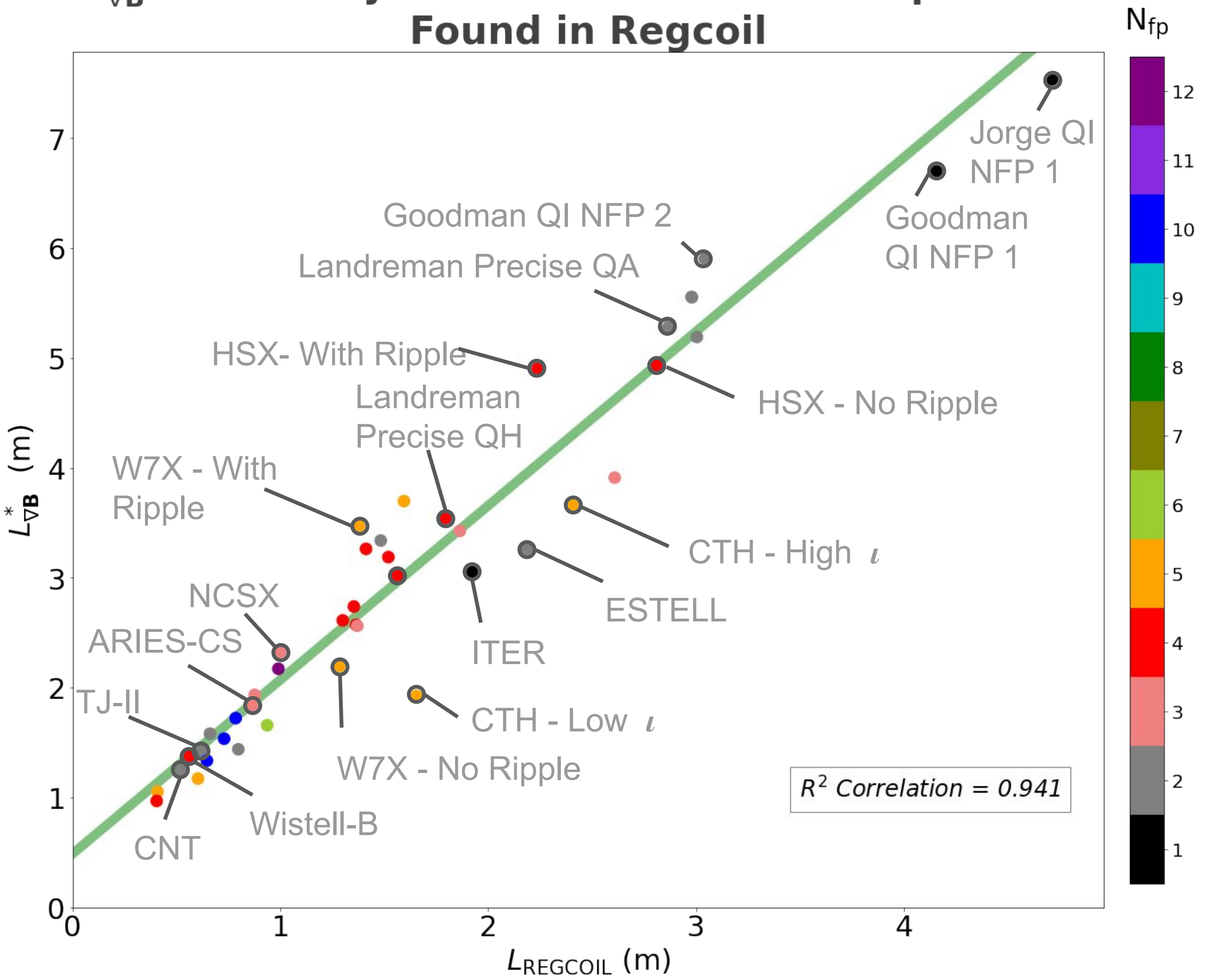

There is Good Spatial Correlation between $||K||_\infty$ and $L^*_{\nabla \mathbf{B}}$

The smallest $L_{\nabla \mathbf{B}}$ and the largest K are located at the same coordinates

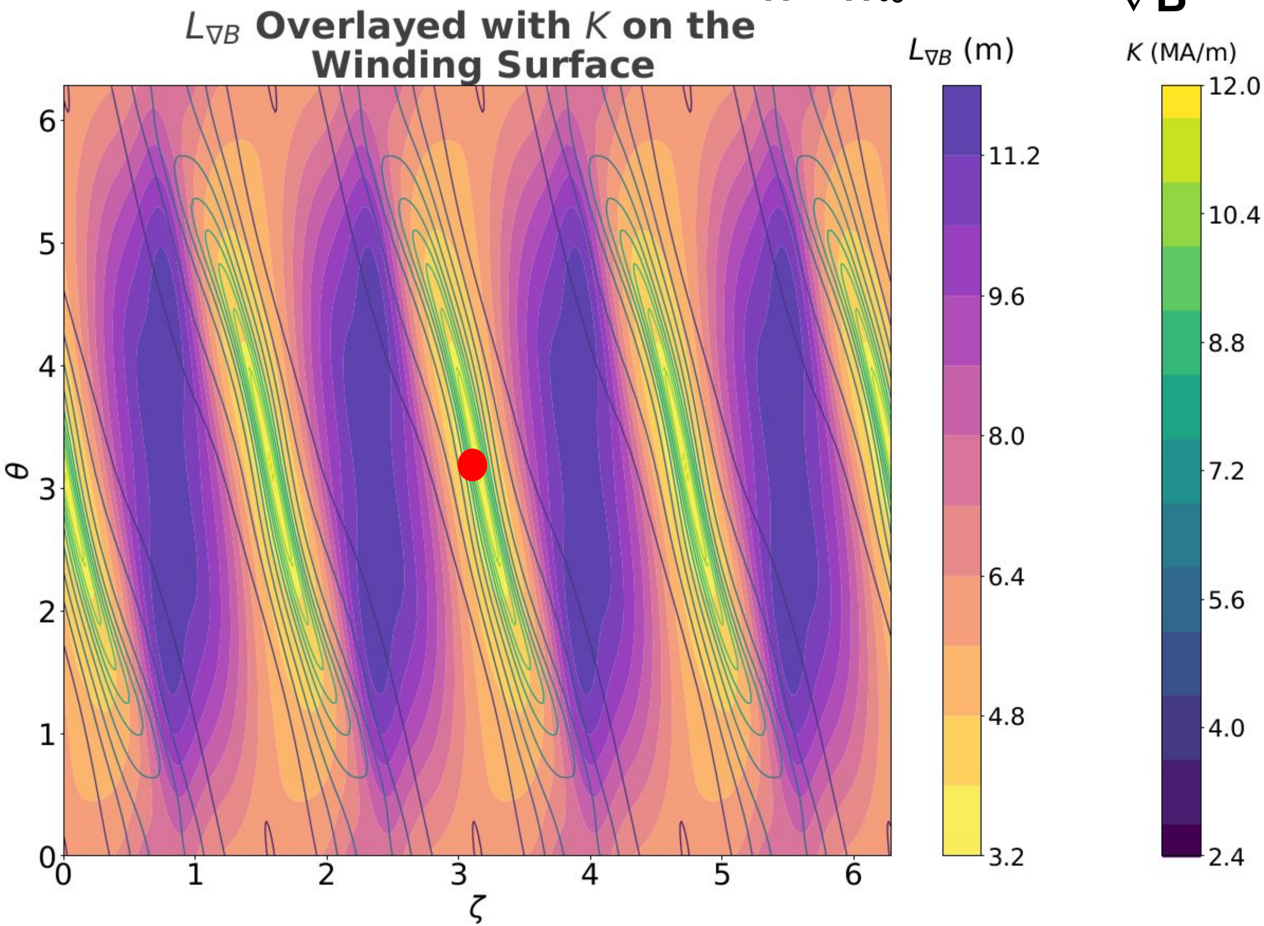

$L_{\nabla B}$ is Shortest on the Inside of the Bean Cross-Section

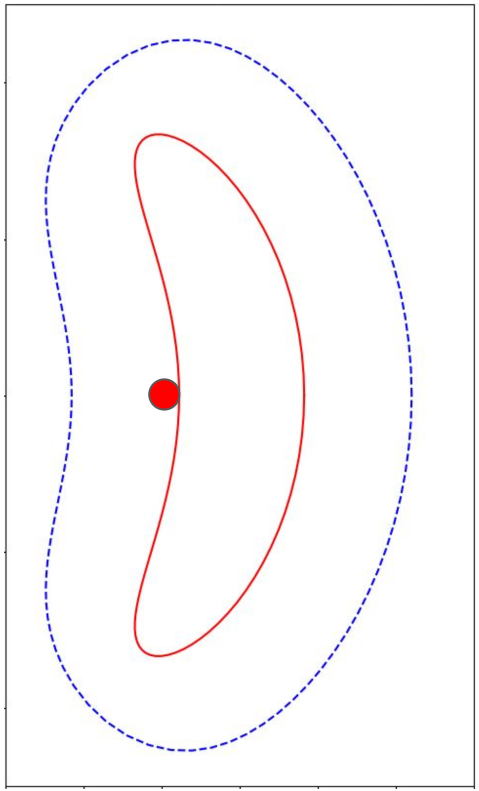

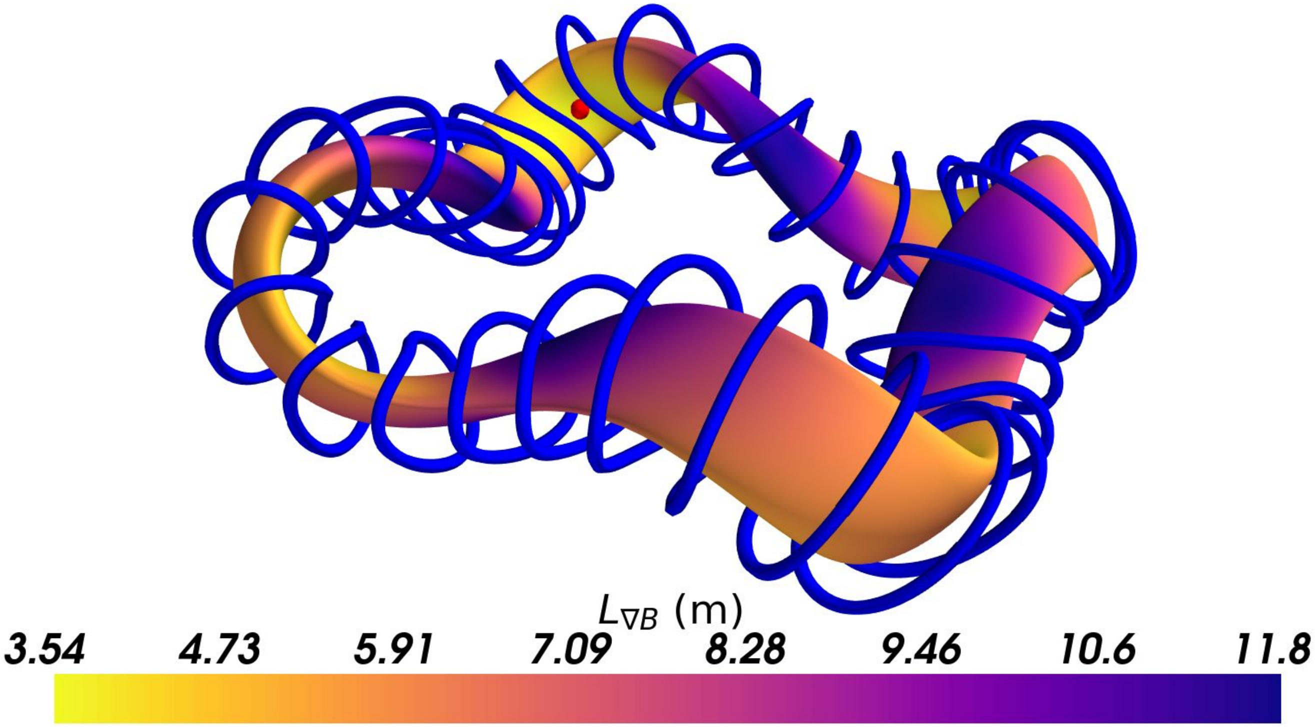

Alternative Magnetic Gradient Scale Lengths are Similar to $L_{\nabla \mathbf{B}}$

$$L_{\mathbf{b}\cdot\nabla\mathbf{b}} = \frac{1}{\|\mathbf{b}\cdot\nabla\mathbf{b}\|},$$

$$L_{\nabla|B|} = \frac{B}{\|\nabla B\|},$$

$$L_{\|\sigma\|} = \frac{\sqrt{2}B}{(\Sigma_i \sigma_i^2)^{1/2}},$$

$$L_{\mathrm{Max}\sigma} = \frac{B}{\mathrm{Max}[\sigma_i]},$$

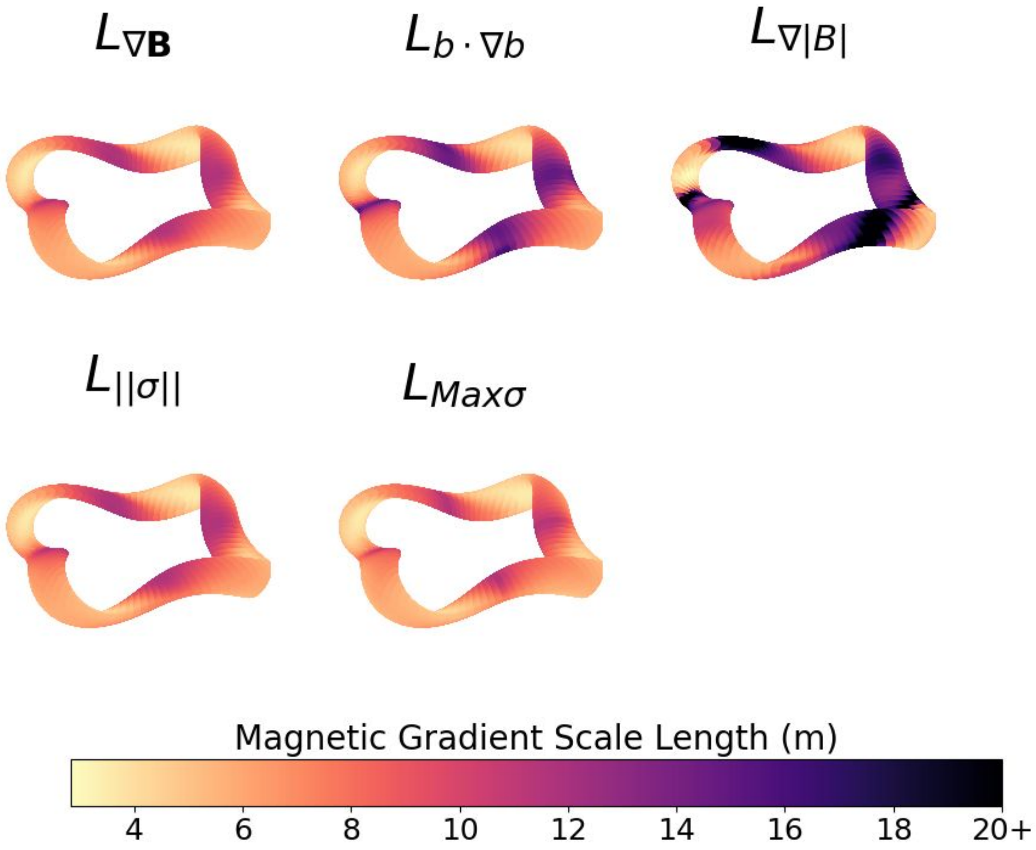

Where σ represents the singular values of $\nabla \mathbf{B}$

Alternative Scale Lengths

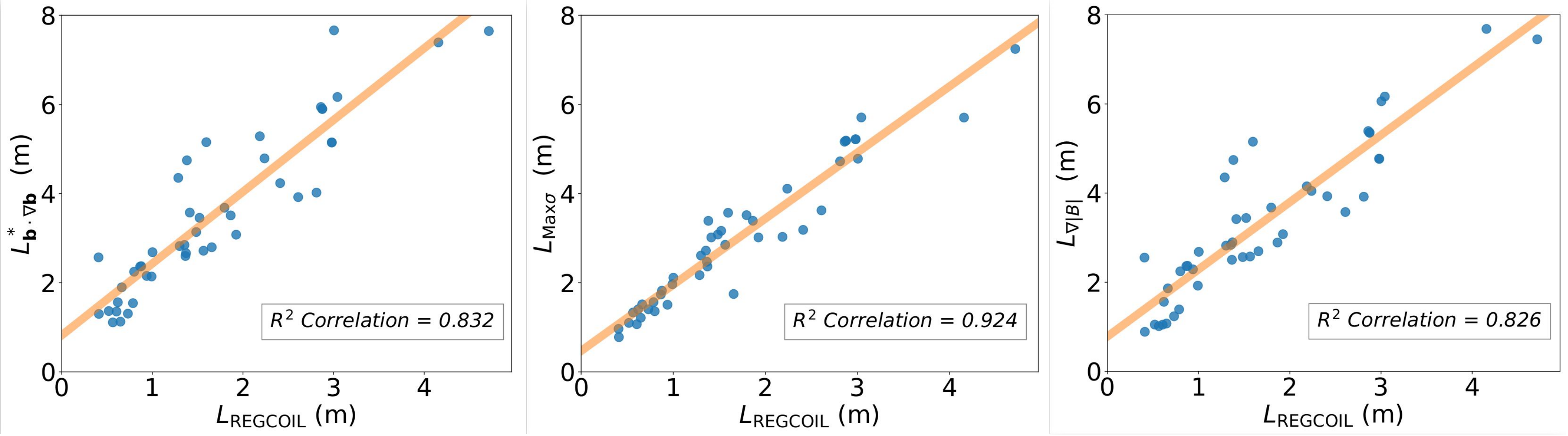

Configurations with High Coil Ripple are Outliers

$$R(\theta, \zeta) = \sum_{m,n} R_{m,n} cos(m\theta - n\zeta)$$

$$Z(\theta, \zeta) = \sum_{m,n} Z_{m,n} sin(m\theta - n\zeta)$$

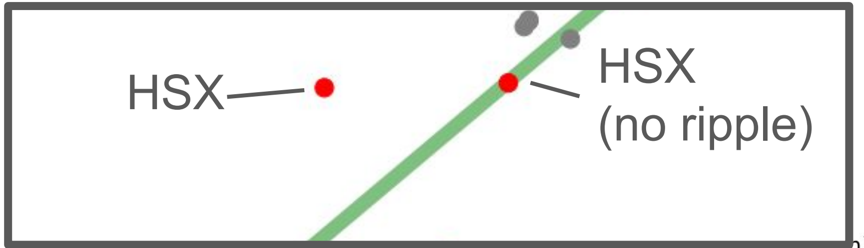

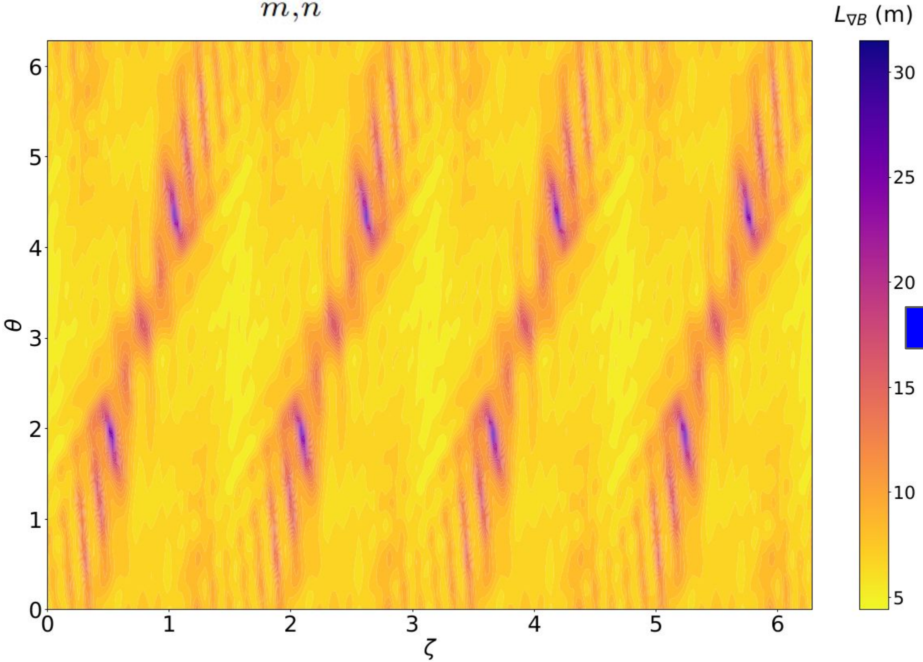

HSX

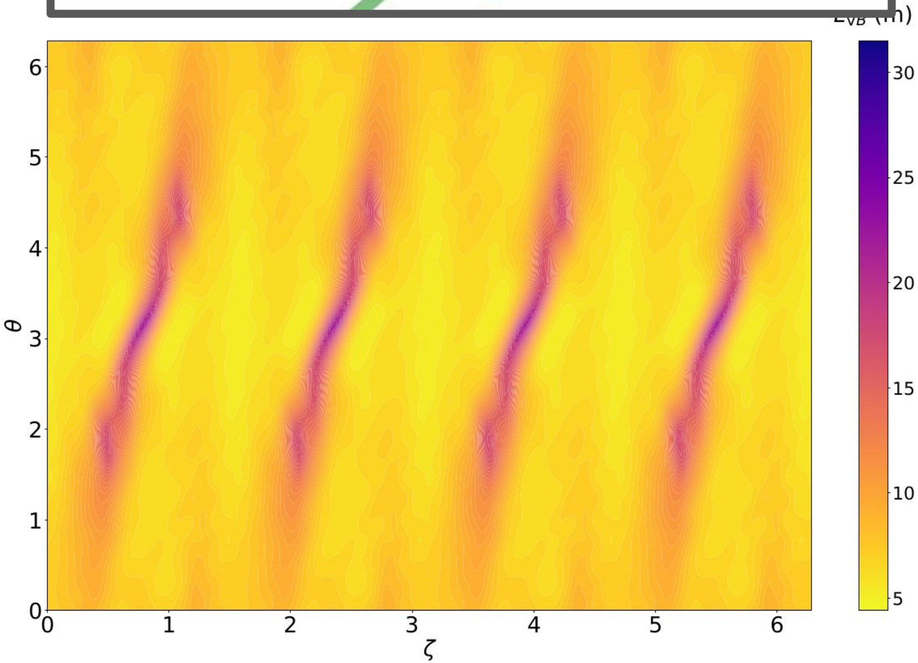

HSX without ripple (n_{max} =4)

Summary

We established a fundamental connection between $L_{\nabla B}$ and the plasma-coil separation. We calculated the distance of $L_{\nabla B}$ of over 40 configurations, and found a strong correlation between $L_{\nabla B}$ and the plasma-coil separation of stage II optimized configurations with magnetic field accuracy and coil complexity constrained.

$L_{\nabla B}$ is shortest on the inside curve of the bean-shaped cross-section of the plasma, which appears to explain why some stellarators are hard to make with distant coils.

Open Questions/ Ongoing Research

1. Can we get better configurations by optimizing for $L_{\nabla \mathbf{B}}$?
    a. Currently Ongoing in DESC
2. Is there a better Magnetic Gradient Scale Length than $L_{\nabla \boldsymbol{B}}$?

$$L_{\nabla\nabla\mathbf{B}} = \frac{4\|\nabla\mathbf{B}\|_F}{\sqrt{2}\|\nabla\nabla\mathbf{B}\|}$$

, where

$$\|\nabla\nabla\mathbf{B}\| = \sqrt{\sum_{i,j,k}(\nabla\nabla\mathbf{B})^2_{ijk}}$$

.

3. How well does $L_{\nabla \mathbf{B}}$ work as a plasma coil separation metric for filamentary coils?
    a. Can we relax the assumptions that we made in REGCOIL?

$||K||_\infty$ is inverse to Minimum Coil-Coil Distance

$$||K|| = \lim_{N\to\infty} \frac{I_{pol}}{Nd_{cc}}$$

$$K_{\max} \equiv ||K||_\infty \approx \frac{I_{pol}}{Nd_{min}}$$

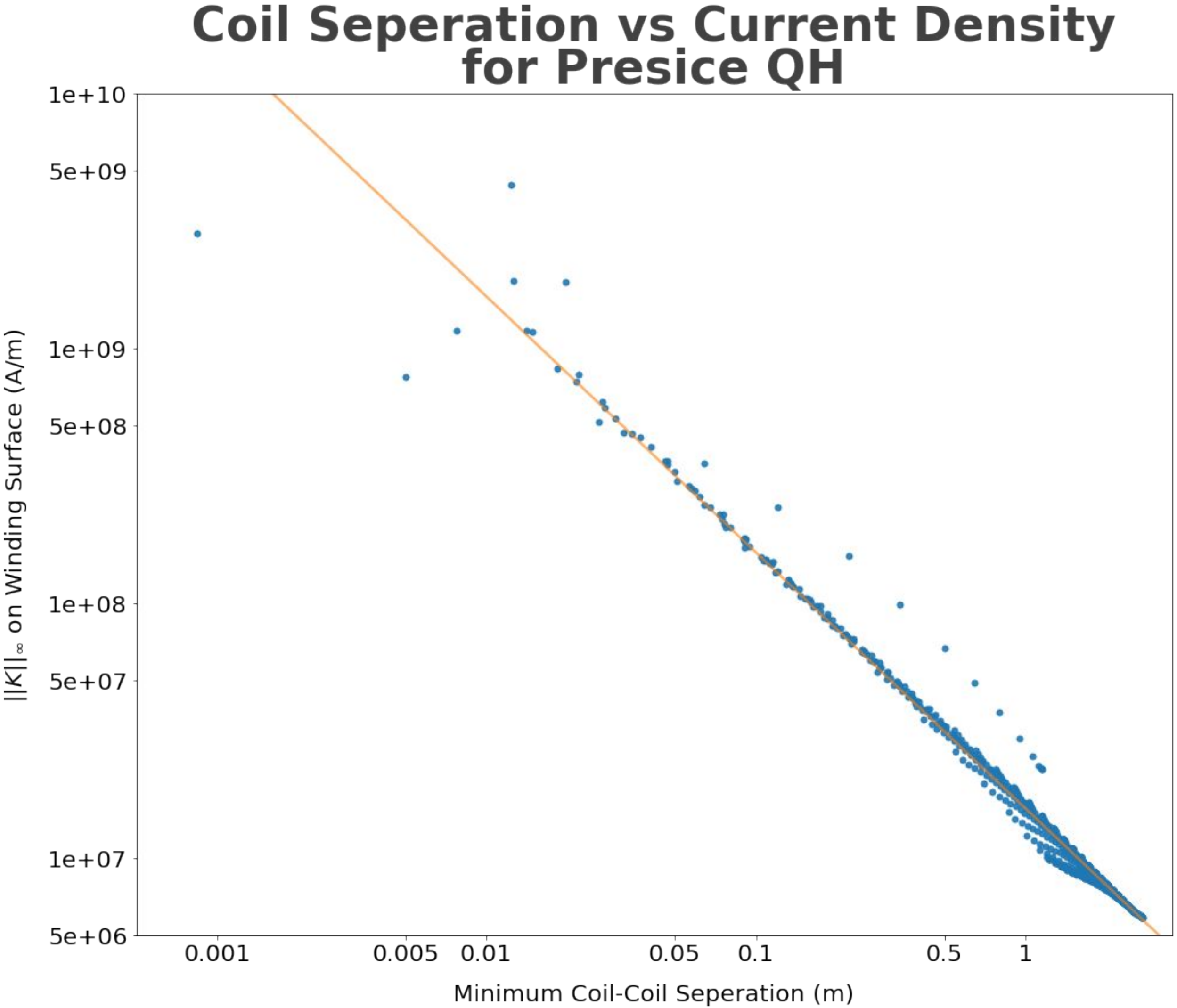

Some `VMEC` Solutions are Inaccurate in Cartesian Coordinates

Outlier configurations do not pass at least one of the following tests. Most likely caused by computer precision error when converting from `VMEC` to Cartesian coordinates

$$\frac{\nabla \mathbf{B} - (\nabla \mathbf{B})^T}{2||\nabla \mathbf{B}||_F} < 0.38$$

This implies that better accuracy can be achieved by either
a) more accurate `VMEC` solutions

b) Finding the Frobenius norm without converting to Cartesian coordinates

Full Table of Plasma Configurations (1/2)

Description	N_{fp}	$\beta(\%)$	$L_{\mathtt{REGCOIL}}$ (m)	$L^*_{\nabla\mathbf{B}}$ (m)
nfp=4 quasi-helical (QH) configuration by Ku & Boozer[43]	4	4.00	0.4060	0.9691
Unpublished QH configuration from Michael Drevlak	5	3.92	0.4099	1.0538
Columbia Non-Neutral Torus (CNT)[44]	2	0	0.5189	1.2507
Tokamak de la Junta II (TJ-II)[45]	4	0	0.5638	1.3777
Wistell-B, Bader et al.[46]	5	0	0.6047	1.1726
Quasi-axisymmetric (QA) configuration designed by Paul Garabedian[47]	2	3.02	0.6188	1.4214
Large Helical Device (LHD), major radius 3.60m[48]	10	0	0.6475	1.3358
Quasi-Poloidal Stellarator (QPS)[49]	2	2.01	0.6625	1.5812
LHD, major radius 3.53m[48]	10	0	0.7302	1.5354
LHD, major radius 3.75m[48]	10	0	0.7858	1.7226
Henneberg et al. QA[50]	2	3.50	0.7987	1.4390
Advanced Research Innovation and Evaluation Study-Compact Stellarator (ARIES-CS)[1]	3	4.06	0.8655	1.8375
National Compact Stellarator Experiment (NCSX) stage-1 optimization result (known as LI383)[51]	3	4.26	0.8771	1.9343
The first quasisymmetric configuration found[52]	6	4.09	0.9374	1.6582
Advanced Toroidal Facility (ATF)[53]	12	4.48	0.9913	2.1721
NCSX free-boundary (c09r00)[51]	3	4.08	1.0015	2.3233
Wendelstein 7-X (W7-X), without coil ripple[54]	5	4.48	1.2858	2.1941
Landreman, Buller, & Drevlak, QH, 5% beta[55]	4	5.58	1.3009	2.6120
Landreman, Buller, & Drevlak, QH, vacuum[55]	4	0	1.3545	2.7385
Boundary constructed by near-axis expansion. Vacuum QH with nfp=4	3	0	1.3650	2.5722
Goodman et al. Quasi-isodynamic (QI) configuration with nfp=3[56]	4	0	1.3712	2.5633

Full Table of Plasma Configurations (2/2)

Quasi-Isodynamic (QI) configuration from CIEMAT[58]	4	0	1.4130	3.2634
Chinese First Quasiaxisymmetric Stellarator (CQFS)[59]	2	0	1.4839	3.3392
Landreman & Paul, QH with magnetic well[27]	4	0	1.5206	3.1882
Wistell-A. Bader et al.[60]	4	0	1.5641	3.0210
W7-X "high narrow mirror" configuration[61]	5	4.00	1.5952	3.6979
Compact Toroidal Hybrid (CTH) Stellarator, vacuum, with low rotational transform[41]	5	0	1.6556	1.9259
Landreman & Paul, precise QH[27]	4	0	1.7960	3.5418
Unpublished nfp=3 QH	3	0	1.8644	3.4277
Up-down-symmetric ITER-like configuration[39]	1	2.28	1.9248	3.0531
Evolutive Stellarator of Lorraine (ESTELL)[62]	2	0	2.1860	3.2610
Helically Symmetric Experiment (HSX), standard configuration, vacuum, with coil ripple[40]	4	0	2.2377	4.9052
Compact Toroidal Hybrid (CTH) stellarator, vacuum, with high rotational transform[41]	5	0	2.4102	3.6607
Boundary constructed by near-axis expansion. Vacuum QH with nfp=3[24]	3	0	2.6091	3.9118
HSX, standard configuration, vacuum, without coil ripple	4	0	2.8111	4.9336
Vacuum QA configuration with 16 coils from Giuliani et al. Coil length 24m.[63]	2	0	2.8602	5.2643
Landreman & Paul, precise QA[27]	2	0	2.8748	5.2977
Wechsung et al. QA without magnetic well, coil length 24m.[64]	2	0	2.8750	5.3037
Wechsung et al. QA with magnetic well, coil length 24m[64]	2	0	2.9790	5.5563
Landreman & Paul QA with magnetic well.[27]	2	0	2.9806	5.5532
Goodman et al. Quasi-isodynamic configuration with nfp=2[56]	2	0	3.0045	5.1919
Landreman, Buller & Drevlak, QA, 2.5% beta[55]	2	2.55	3.0419	5.9042
Goodman et al. Quasi-isodynamic configuration with nfp=1[56]	1	0	4.1563	6.6993
Jorge et al. Quasi-isodynamic configuration with nfp=1[65]	1	0	4.7133	7.5360

$L_{\nabla \mathbf{B}}$ Behavior In A Circular Wire

$$\rho^2 = x^2 + y^2;\; r^2 = x^2 + y^2 + z^2;\; \alpha^2 = 1 + r^2 - 2\rho$$

$$\beta^2 = 1 + r^2 + 2\rho;\; k^2 = 1 - \frac{\alpha^2}{\beta^2}$$

$$B_x = \frac{x}{2\alpha^2\beta\rho^2}[(1+r^2)E(k^2) - \alpha^2 K(k^2)]$$

$$B_y = \frac{y}{2\alpha^2\beta\rho^2}[(1+r^2)E(k^2) - \alpha^2 K(k^2)]$$

$$B_z = \frac{1}{2\alpha^2\beta}[(1-r^2)E(k^2) + \alpha^2 K(k^2)],$$